Mersin Photogrammetry Journal

https://dergipark.org.tr/en/pub/mephoj

e-ISSN 2687-654X

3D reconstruction of foot metatarsal bones of women using CT images

Hatice Çatal Reis *[1]

[1] *Gümüşhane University, Department of Geomatics Engineering, Türkiye, hcatal@gumushane.edu.tr*

Cite this study: Reis, H. Ç. (2024). 3D reconstruction of foot metatarsal bones of women using CT images. Mersin Photogrammetry Journal, 6 (1), 32-38

https://doi.org/10.53093/mephoj.1435928

Keywords
Metatarsal
CT-scan images
Medical photogrammetry
3D reconstruction
Medical image processing

Research Article

Received:12.02.2024
Revised: 10.03.2024
Accepted: 14.03.2024
Published:16.03.2024

Abstract

Bone morphology is a fundamental factor in human anatomy. However, foot and ankle bones have yet to be adequately evaluated in 3-dimensional. It is essential to present the biometric data of anatomical structures. This study formed 3D models of the metatarsal bones of the feet of young women using image processing techniques to examine biometric measurements and determine morphology on these 3D models. This study investigated bone lengths in the metatarsal bones of women feet in Türkiye. A total of ten young female subjects were included as the test group to measure the lengths of their foot metatarsal bones using CT (Computed Tomography) scans, and 20 feet (left/right) were examined. The parameters that were used for the analyses were detector collimation of 64x0.5 mm, section thickness of 0.5 mm, current of 100 mA, tube voltage of 120 kVp, and pixel spacing of 512x512 pixels with a monochrome resolution providing 16-bit gray levels. CT images were processed, and a 3D metatarsal reconstruction was gathered. Then, the biometric measurements were calculated on this 3D model. For the lengths of the volunteers' right/left foot metatarsal bones, statistically significant differences were calculated using a one-sample t-test. For the female metatarsal bones of the left and right feet, statistically significant differences in length were calculated on 3D models. The mean results of the metatarsal length measurements were MT1(metatarsal): 59.52±1.42 mm, MT2: 70.45±1.82 mm, MT3: 66.25±1.82 mm, MT4: 65.12±1.81 mm and MT5: 63.63±1.81 mm. The level of statistical significance was accepted as $p < 0.05$ for the one-sample t-test conducted for each metatarsal bone. The lengths of the right foot metatarsal bones were different from those of the left foot metatarsal bones in the sample. However, this difference was approximately one-tenth of a millimeter. The shortest bone was MT1, and the longest bone was MT2. These measurements are consistent with the anatomical information in the literature. The 3D models from the CT images and the biometric measurements of the metatarsal bones were found to be reliable and accurate.

1. Introduction

Medical photogrammetry has been used for decades to measure, model, or provide metric data on various parts of the body. Medical photogrammetry uses medical images to produce this data/information. Computer Tomography images of women's foot metatarsal bones have been used in this research. According to the Turkish Statistical Institute, the female population in Türkiye was 49.8% of the total population in 2018, and nearly 6.344 million of women were considered as young women. Metatarsal fractures are the most common foot injuries investigated in the literature [1-4], and, according to the reports, fractures between 67 and 75.4/100,000 per year [5]. Approximately 40% of injury patterns in dancers are observed in the lower leg, foot, and ankle [6]. The metatarsal bones of the human foot consist of five bone units, and metatarsal fractures in dancers' feet are usually seen in the second and fifth bones [7]. These dancers' bones are usually broken when they miss a step or are in a point state [8]. In some cases, it becomes challenging for doctors to determine stress fractures [9,10]. The9% of metatarsal fractures occur in athletes and sports [4]. Additionally, metatarsals are important in hallux valgus, which has a negative impact on gait mechanics [11]. The best treatment for this condition is still challenging [12]. The effect of the first metatarsal osteotomy on the midfoot bones in patients with hallux valgus was investigated [13]. What should be considered here is the ability to accurately detect any fracture, deformation, or anomaly through early diagnosis and treatment. It is of vital that athletes, dancers, or people can quickly return to their daily routines such as, sport, and dancing. Metatarsal researches are rarely studied in the current literature, generally focusing on treatment recommendations [5]. Comprehensive research for the

metatarsal bones is necessity [14]. 3D modelling provides an essential opportunity for overcoming such difficulties. With the assistance of various programs developed in recent years, 3D images are generated from instant 2D images, which are taken as intersections of parallel fields along relevant objects such as feet covered in this research. It is possible to use 3D modeling software for vector-based 3D geometric modeling, which conforms to the definition of tissue-bound geometry beyond the 3D display of tissues [15-17]. Researchers are developing various modelling methods, such as the repeatable kinematic multi–segment model [18]. In the literature, several techniques for 3D bone measurements have been introduced, allowing area, volume, surface, distance, and angular measurements of 3D models generated from CT or MRI images [18-21]. A study investigated bone morphology by creating a 3D model of rare foot disorders using MRI images [22]. Computer-aided design (CAD) [23] and Computer-assisted tomography (CAT), diagnosis [24], pre-operative planning, surgical navigation, and surgical processes have been used in the surgical management of such cases. CAD has supported detection and can improve the diagnosis for radiologists [25]. CT devices have been known as the best technique for bone imaging since the 1970s. With its resolution and 3D capability, the CAT scan images substantially revolutionized the medicine area. A series of CAT sectional images are obtained by moving the CT device vertically in the longitudinal direction. The device takes these images in large quantities depending on the resolution of the 3D longitudinal scan. Sections are then generated to form a 3D model [26]. Multi-detector Computed Tomography (MDCT) images may be used to design the subtalar prostheses and analyse surgical procedures of the ankle and the hindfoot [27]. 3D CT images of the bones create surface meshes, and bone angles are measured [19]. The creation and evaluation of 3D models for morphological calculations of human bones still need to be sufficiently done. There is still a need for new research and studies in this field. In this experimental research, after obtaining the 3D models of the women's metatarsal foot bones, the biometric measurements were taken, and deformations became detectable using image processing techniques.

The 3D models formed in this study were created using CT images. 3D rendering of metatarsals was used to diagnose disorders and to make morphological measurements of the metatarsal bones.

After reviewing the recent literature, we found a few pieces of research about the foot that employ biomedical measurements. Previous studies have usually focused on the shape and characteristics of the foot [28-31]. The study [21] designed a method for 3D morphological measurements of the normal calcaneus based on CT image processing techniques. Another study presented a semi-automatic segmentation approach for biometric measurement of the talus bone using CT images [32]. This study aimed to introduce a method for 3D morphological measurements of the metatarsal bones based on CT pre/post-processing techniques and measure biometric parameters in a female case. The research provides information about biometric measurements of the metatarsal bones of young women in Türkiye. This research constructed 3D models of the metatarsal bones of healthy female volunteers. The method studied here is expected to speed detection of the diagnosis and treatment in different medical fields, such as orthopedics, surgery, anatomy, sports medicine, and veterinary medicine. Thus, medical standards may be reachable, and repeatable measurements may be taken confidingly. 3D models provide a general and computationally efficient solution for biometric measurements and are suitable for the real-time modelling. Moreover, this study may provide a helpful information for developing foot—and ankle-related products or improving orthopedic footwear design for women and men. Additionally, for educational purposes, 3D bone modelling techniques may be used in anatomy classes and physical training at colleges.

2. Material and Method

This study employed 3D models of the metatarsal foot bones of Turkish women born in 1992 for the analysis of differences between the left and right foot using digital image processing techniques. MDCT images of 20 feet were examined and about 12000 CT images were processed. The general demographic data of the subjects were investigated, and the sample's mean age was 18, their mean shoe size was 37±1.2, their mean height was 165±8 cm, and their mean weight was 49.8±4.2 kg.

2.1. CT scans and image processing

During the scanning process, the health of the volunteers was considered as top priority of this study. This study was therefore carried out by paying a great attention to the standards of the existing procedures of the Declaration of Helsinki [33] and the Turkish Society of Radiology Computed Tomography Regulation [34] in accordance with the Clinical Research Ethics Committee documents (Decision No. 004,08/01/2010) to avoid the negative impacts on the volunteers participated in this study.

The participants were carefully selected from among those with no orthopedic disorders or a history of orthopedic disorders and women with no history of professional dancing or sports. The axial CT images of the volunteers were taken, and the metatarsal bones of the right and left feet were tested. A total of 20 feet were analysed in the study. The doses of radiation were adjusted within the allowed range, with respect to the scan parameters that do not harm the volunteers' health, and these experiments were conducted under experienced radiologist supervision. Additional parameters were applied to reduce the dose even further. The participants' feet were scanned side by side or separately using the CT device. The same image and scanning parameters were used for all the scanning process. To increase the accuracy of each image obtained by the MDCT device, the feet of the volunteers were fixed to the table to keep them still. The scans were carried out by high-resolution CT (Toshiba Aquillon, America Medical Systems). The parameters were 64x0.5 mm - 4x0.5 mm for detector collimation, 0.5 mm for section thickness, 100 mA of current, a tube voltage of 120 kVp, a matrix of 512x512 pixels for pixel spacing, and 16-bit

grey levels for monochrome resolution. When scanning the CT images, great attention was paid to getting the images with a minimal, harmless dose of radiation but with high resolution. Cross-section images were acquired and stored in the Digital Imaging and Communications in Medicine (DICM) format and then imported into the computer environment with a 3D analysis software called "3D-Doctor". Following this, 3D models were generated. The model's geometry was obtained from 3D reconstruction of the CT images of healthy female volunteers' left and right feet. These 3D models of the women's metatarsal bones were used for the biometric measurements.

All measurements were taken separately for the right and left feet. The 3D reconstructions of the metatarsal bones and the biometric measurements were calculated using the 3D-Doctor. $p<0.05$ was considered as critical value for statistical significance.

2.2. 3D Modelling

Two different techniques are usually performed for displaying 3D data. These are the volume and surface rendering techniques. In surface rendering, objects with a smooth geometry are expressed by the continuous functions. An exact function cannot define objects with non-specific geometry; instead, these surfaces are expressed as the definitions of small surface elements [35]. In volume rendering, the voxel values are determined by monitoring the rays passing through each voxel throughout the volume, or voxels on the object are processed by back-to-front or reverse transactions [35]. The axial images in the .dcm format were first imported to a computer with 3D modeling software, and calibration was automatically performed by the software. While processing the images, a median filter was applied to remove the spot or line noise in the CT images. The bone and non-bone materials were defined in each CT slice as Hounsfield Units. Hounsfield unit is determined as variable values between 32900-40000. Segmentation was performed to classify the pixels showing the same characteristics on the MDCT images. To create a surface model, object boundaries must be identified. This study utilized the region-growing segmentation method. The Hounsfield scale was also used for the interactive segmentation (Figure 1).

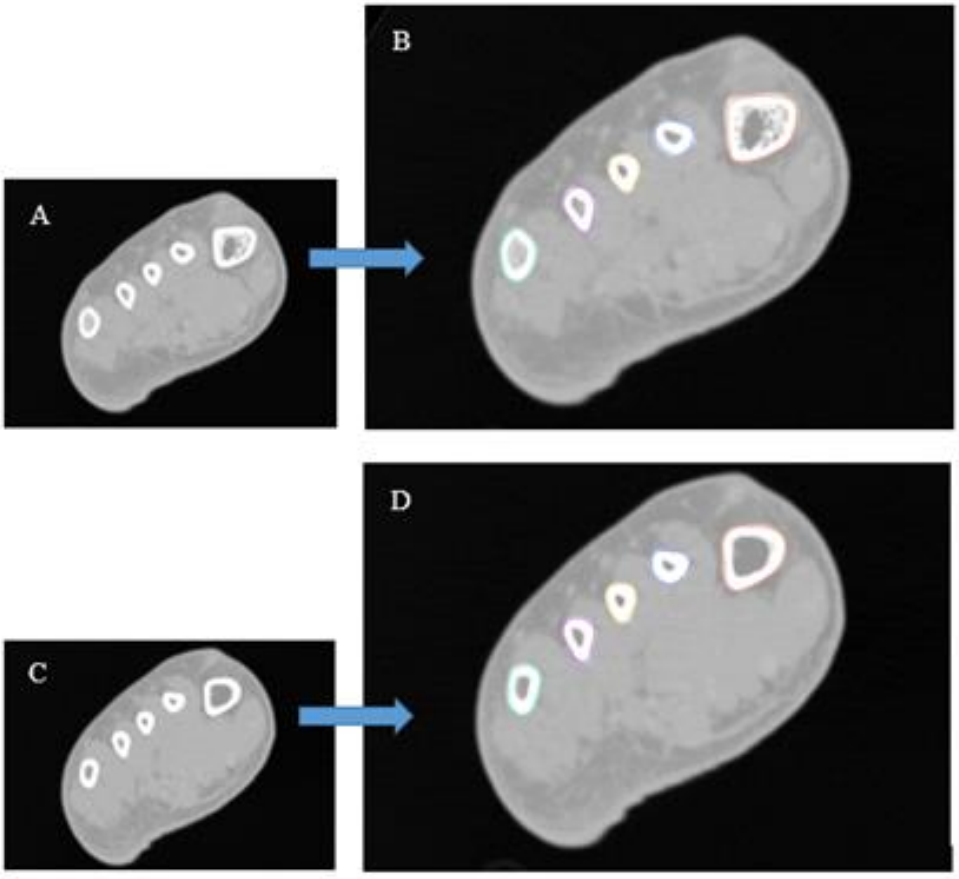

Figure 1. Demonstration of segmentation result of raw slices.

*A/C: raw CT slices, B/D: an interactive and automatic segmentation technique was applied to distinguish all components of the metatarsal bones.

The 3D structures of each metatarsal bone were reconstructed by shaded surface display (SSD) with a reconstruction. With the assistance of the perspective icon of SSD reconstruction, the defined boundary of the surface could be observed. Then, the metatarsal bone was generated and detected (Figure 2). Each length was calculated by the software (yellow line) (Figure 2).

Thus, the 3D models of the metatarsal bones were then generated individually as separate models in separate layers (Figure 3).

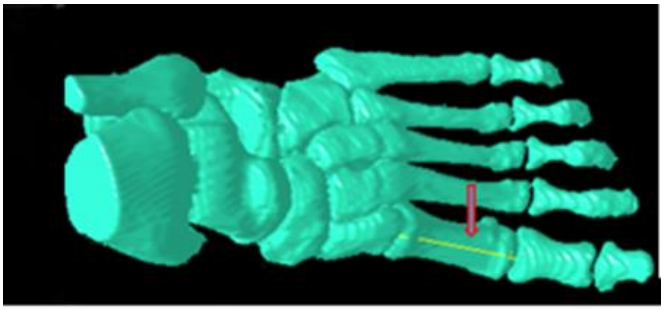

Figure 2. 3D-reconstructed images of the metatarsal bones in a woman foot and biometric measurement.

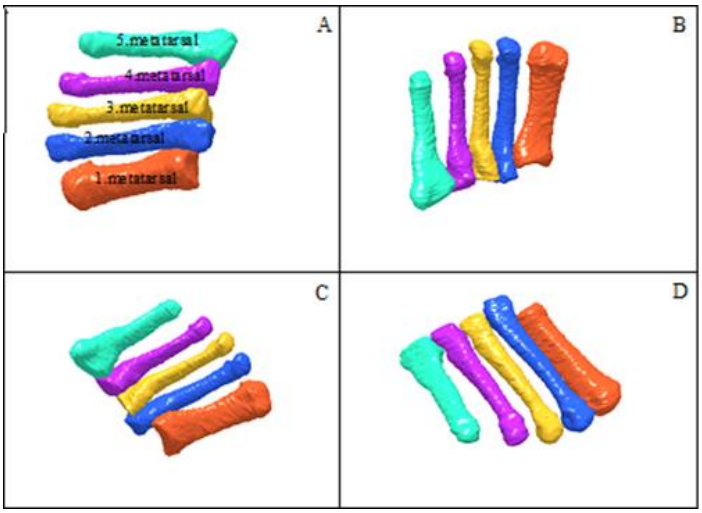

Figure 3. Reconstruction of 3D metatarsal bones.

*A/D: After the segmentation, the SSD reconstruction image of the 3D metatarsals presented the anterior. B/C: Posterior view of 3D model Biometric measurements were made on these models, and calculations were carried out using these measurements. The 3D measurement process was carried out as follows (Figure 4):

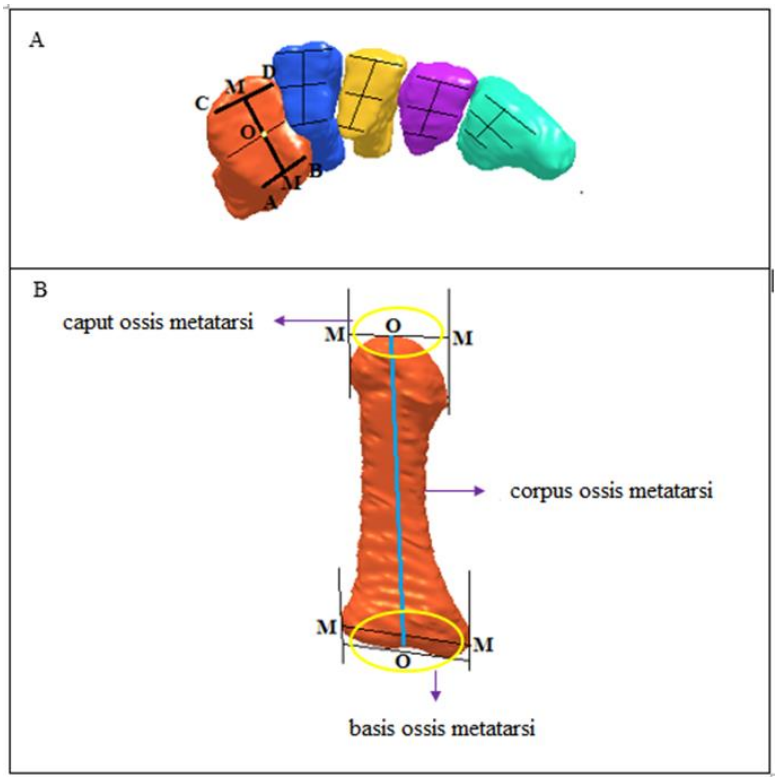

Figure 4. Three-dimensional morphological measurements of metatarsal bones.

Lengths from the caput ossis metatarsi to the basis ossis metatarsi were calculated. 4a, the length of M: the midpoint between A and B/ C and D, Figure 4a-4b, the height of the O: distance between M_1 and $M_2/2$.

2.3. Statistical analysis

The research methods include a qualitative analysis and quantitative measurement. Statistical analyses were performed in MATLAB. One-sample t-test was used to determine whether a sample from a population with a specific mean. Therefore, the mean length of the metatarsals of women were not always known, but sometimes hypothesised. The one-sample t-test for the non-parametric samples was applied to determine whether or not there were significant differences in the metatarsal bones' lengths in young women in Türkiye. $p<0.05$ was considered to be statistically significant for the one-sample t-test of each metatarsal bone. The alpha level was chosen as 5% (0.05) in the study. If the test result is a small p (≤ 0.05), this is strong evidence that the null hypothesis is invalid. If the test result is a large p (> 0.05), it means that the alternative hypothesis is weak, so the null hypothesis cannot be rejected. The mean parameters for all measurements for the lengths and the standard errors of mean (SEM) were calculated using the formulae below.

Arithmetic mean (Equation 1-2);

$$\bar{X} = \frac{X_1 + X_2 + \cdots X_n}{n} \quad (1)$$

$$\bar{X} = \frac{\sum X_i}{n} \quad (2)$$

i: 1, 2, 3

Standard deviation (Equation 3);

$$S = \sqrt{\frac{\sum (X_i - \bar{X})^2}{n}} \quad (3)$$

Standard error refers to the error of the sample mean (Equation 4).

$$SEM = \frac{S}{\sqrt{n}} \quad (4)$$

Sample mean is expressed with standard error (Equation 5-6).

$$\bar{X} + S_{\bar{X}} \quad (5)$$

$$Mean \pm SEM \quad (6)$$

One-sample t-test was performed (Equation 7).

$$t = \frac{X - m_0}{S_{\Delta_x}} \quad (7)$$

The bone lengths of the metatarsus-1, 2, 3, 4 and 5 were combined. The measurement value of each bone was obtained. The lengths of all bones in the right and left metatarsal bones in the sample were calculated. Their significance was examined in the one-sample t-test, and deformation analyses were thus performed. The same statistical processes were carried out for all the participants. The biometric values of the metatarsal bones in the left feet are given in Table 1.

Table 1. 3D biometrical parameters of metatarsal bones of the left foot.

Left foot	MT1 (mm)	MT2 (mm)	MT3 (mm)	MT4 (mm)	MT5 (mm)
1	53.68	65.78	61.88	59.24	63.16
2	58.98	69.41	62.38	61.95	57.76
3	54.68	66.98	62.58	60.04	64.56
4	59.58	69.99	63.08	62.25	58.36
5	58.96	66.98	63.19	63.10	58.00
6	60.36	73.27	68.32	66.98	66.93
7	61.12	72.93	65.80	66.59	65.94
8	63.00	75.68	71.47	69.75	67.37
9	62.43	75.89	73.86	71.36	68.96
10	62.33	72.54	67.94	67.68	64.79
mean	59.51	70.95	66.05	64.89	63.58

*MT1: metatarsal 1, MT2: metatarsal 2, MT3: metatarsal 3, MT4: metatarsal 4, MT5: metatarsal 5. The biometric values of the metatarsal bones in the right foot are given in Table 2. Table 2. 3D biometrical parameters of the metatarsal bones in the right foot.

Table 2. 3D biometrical parameters of metatarsal bones of the right foot.

Right foot	MT1 (mm)	MT2 (mm)	MT3 (mm)	MT4 (mm)	MT5 (mm)
1	53.69	63.92	63.92	61.32	62.01
2	59.02	67.12	62.01	62.00	60.37
3	54.99	65.82	64.92	62.32	63.01
4	59.99	68.12	63.23	62.00	60.69
5	58.58	65.47	63.35	62.25	56.75
6	60.76	73.61	68.46	67.92	66.87
7	61.12	72.93	65.80	66.59	65.94
8	63.01	75.06	71.17	70.32	67.50
9	62.15	75.22	73.47	71.06	68.70
10	61.99	72.21	68.10	57.58	64.94
mean	59.53	69.95	66.44	65.34	63.68

3. Results

For the metatarsal bones of the female left and right feet, statistical differences were calculated for the length of the 3D models. When the left feet of the participants were evaluated, human subject 8 had the longest foot length in the first metatarsal, while human subject 1 had the shortest length. In the second metatarsal, the ninth human subject has the largest length, while the first has the smallest value. While the ninth human subject has the largest length in the third and fourth metatarsals, the first human subject has the smallest value. Subject 2 had the smallest length in the fifth metatarsal, while human subject 9 had the largest length. When evaluating the participants' right feet, human subject 8 had the longest foot length at the first metatarsal, while human subject 1 had the shortest foot length. In the second metatarsal, human subject 9 has the largest length, while human subject 1 has the smallest value. While subject 9 has the largest length in the third metatarsal, human subject 2 has the smallest value. While subject 9 has the largest length in the fourth metatarsals, human subject 1 has the smallest value. Subject 2 had the smallest length at the fifth metatarsal, while human subject 9 had the largest length. The metatarsal lengths were obtained as

following: MT1: 59.52±1.42 mm, MT2: 70.45±1.82 mm, MT3: 66.25±1.82 mm, MT4: 65.12±1.81 mm, MT5: 63.63±1.81 mm. The shortest bone was MT1, and the longest bone was MT2. The data adhered to a normal distribution. We used one-sample Kolmogorov-Smirnov test for MT1: 0.096, MT2: 0,115, MT3: 0.109, MT4: 0.05, MT5: 0.2. The basic null hypothesis was that the population mean was equal to a hypothesised value,

H_0: μ_0 = Hypothesised value.

The one-sample t-test results and technical details are presented in the following order:

$P_{m1}<0.999$, $P_{m2}<0.997$, $P_{m3}<0.997$, $P_{m4}<0.995$, $P_{m5}<1$

A statistically significant difference was observed based on normal distribution.

4. Conclusion

Medical photogrammetry is applied in the measurements and calculations of many organs. This research focused on the morphometry of the foot metatarsal bone using the medical photogrammetric technique. Metric values were produced and presented on the 3D models of the metatarsal bones. The metatarsal bones of women were examined in this study. While the length value of each people worldwide is unique, the foot anatomies of the two feet (left/right) are also different than each other. Right-foot metatarsal bones are longer than left-foot metatarsal bones. However, this difference is about one-tenth of a millimetre. The main reason for this difference may be that the volunteers have a right dominant side. The statistical and biometric measures on the right and left feet of the participants were performed and analysed in detail. The results of this study and the measurements were analysed unbiased. Medical professionals make calculations using an imaging network/database or by directly reaching the bone. The reliability of these measurements and calculations depends on the expert's experience and knowledge. Minimizing the negative impact of human activity is crucial in this process. The 3D morphological measurements based on CT image processing were highly reliable and repeatable for the anatomic and morphological measurements of the metatarsals. This technique will be helpful for the anatomic reduction of metatarsal fractures and anomalies. Hence, this study underlined that doctors may benefit from pre-generated 3D models for the diagnosis and treatment related to metatarsal bones in such cases. This study contributes to high-accuracy visualization in areas such as anthropology, sports and dance injuries, anatomical training, forensic identification, orthopedics, and surgery. The results may be extended and become transferable for the other cases by increasing the number of participants in further studies.

Acknowledgement

The author is grateful to Selcuk University, Scientific Research Project Coordination for their technical help (Project No: 10101011).

Conflicts of interest

The authors declare no conflicts of interest.

References

1. Spector, F. C., Karlin, J. M., Scurran, B. L., & Silvani, S. L. (1984). Lesser metatarsal fractures. Incidence, management, and review. Journal of the American Podiatric Medical Association, 74(6), 259-264. https://doi.org/10.7547/87507315-74-6-259
2. Polzer, H., Polzer, S., Mutschler, W., & Prall, W. C. (2012). Acute fractures to the proximal fifth metatarsal bone: development of classification and treatment recommendations based on the current evidence. Injury, 43(10), 1626-1632. https://doi.org/10.1016/j.injury.2012.03.010
3. Cakir, H., Van Vliet-Koppert, S. T., Van Lieshout, E. M. M., De Vries, M. R., Van Der Elst, M., & Schepers, T. (2011). Demographics and outcome of metatarsal fractures. Archives of orthopaedic and trauma surgery, 131, 241-245. https://doi.org/10.1007/s00402-010-1164-6
4. Beddard, L., Roslee, C., & Kelsall, N. (2024). Acute and stress fractures of the metatarsals in athletes. Orthopaedics and Trauma, 38(1), 46-50. https://doi.org/10.1016/j.mporth.2023.11.008
5. Herterich, V., Hofmann, L., Böcker, W., Polzer, H., & Baumbach, S. F. (2023). Acute, isolated fractures of the metatarsal bones: an epidemiologic study. Archives of Orthopaedic and Trauma Surgery, 143(4), 1939-1945. https://doi.org/10.1007/s00402-022-04396-3
6. Macintyre, J., & Joy, E. (2000). Foot and ankle injuries in dance. Clinics in Sports Medicine, 19(2), 351-368. https://doi.org/10.1016/S0278-5919(05)70208-8
7. Lee, H. A., Batley, M. G., Krakow, A., Buczek, M. J., Sarkar, S., Talwar, D., ... & Davidson, R. S. (2023). New Classification for Pediatric Proximal Fifth Metatarsal Fractures. The Journal of Foot and Ankle Surgery, 63(2), 267-274. https://doi.org/10.1053/j.jfas.2023.11.015
8. Prisk, V. R., O'Loughlin, P. F., & Kennedy, J. G. (2008). Forefoot injuries in dancers. Clinics in sports Medicine, 27(2), 305-320. https://doi.org/10.1016/j.csm.2007.12.005
9. Goulart, M., O'Malley, M. J., Hodgkins, C. W., & Charlton, T. P. (2008). Foot and ankle fractures in dancers. Clinics in sports medicine, 27(2), 295-304. https://doi.org/10.1016/j.csm.2008.01.002
10. Van Dijk, C. N., & Marti, R. K. (1999). Traumatic, post-traumatic and over-use injuries in ballet: with special emphasis on the foot and ankle. Foot and ankle surgery, 5(1), 1-8. https://doi.org/10.1046/j.1460-9584.1999.51122.x
11. Dygut, J., & Piwowar, M. (2022). Muscular Systems and Their Influence on Foot Arches and Toes Alignment—Towards the Proper Diagnosis and Treatment of Hallux Valgus. Diagnostics, 12(12), 2945. https://doi.org/10.3390/diagnostics12122945

12. Barg, A., Harmer, J. R., Presson, A. P., Zhang, C., Lackey, M., & Saltzman, C. L. (2018). Unfavorable outcomes following surgical treatment of hallux valgus deformity: a systematic literature review. JBJS, 100(18), 1563-1573. https://doi.org/10.2106/JBJS.17.00975
13. Cruz, E. P., Sanhudo, J. A. V., Iserhard, W. B., Eggers, E. K. M., Camargo, L. M., & de Freitas Spinelli, L. (2024). Midfoot width changes after first metatarsal osteotomy in hallux valgus surgery: a biomechanical effect?. The Foot, 102070. https://doi.org/10.1016/j.foot.2024.102070
14. Khurana, A., Alexander, B., Pitts, C., Brahmbhatt, A., Cage, B., Greco, E., ... & Shah, A. B. (2020). Predictors of malreduction in zone II and III Fifth metatarsal fractures fixed with an intramedullary screw. Foot & Ankle International, 41(12), 1537-1545. https://doi.org/10.1177/10711007209474
15. Černochová, P., Kaňovská, K., Kršek, P., & Krupa, P. (2005). Application of geometric biomodels for autotransplantation of impacted canines. World Journal of Orthodontics, 1.
16. Krupa, P., Kršek, P., Černochová, P., & Molitor, M. (2004). 3-D real modelling and CT biomodels application in facial surgery. In Neuroradiology. Berlin: European Society of Neuroradiology, 141, 1. ISBN 0028-3940.
17. Krupa, P., Krsek, P., Javorník, M., Dostál, O., Srnec, R., Usvald, D., ... & Necas, A. (2007). Use of 3D geometry modelling of osteochondrosis-like iatrogenic lesions as a template for press-and-fit scaffold seeded with mesenchymal stem cells. Physiological research, 56(1), 107-114. https://doi.org/10.33549/physiolres.931308
18. Stebbins, J., Harrington, M., Thompson, N., Zavatsky, A., Theologis, T., Repeatability of a model for measuring multi-segment foot kinematics in children. Gait & Posture 2006; 23:4- 401–410. https://doi.org/10.1016/j.gaitpost.2005.03.002
19. Gutekunst, D. J., Liu, L., Ju, T., Prior, F. W., & Sinacore, D. R. (2013). Reliability of clinically relevant 3D foot bone angles from quantitative computed tomography. Journal of foot and ankle research, 6, 1-9. https://doi.org/10.1186/1757-1146-6-38
20. Eckstein, F., Cicuttini, F., Raynauld, J. P., Waterton, J. C., & Peterfy, C. (2006). Magnetic resonance imaging (MRI) of articular cartilage in knee osteoarthritis (OA): morphological assessment. Osteoarthritis and cartilage, 14, 46-75. https://doi.org/10.1016/j.joca.2006.02.026
21. Qiang, M., Chen, Y., Zhang, K., Li, H., & Dai, H. (2014). Measurement of three-dimensional morphological characteristics of the calcaneus using CT image post-processing. Journal of foot and ankle research, 7, 1-9. https://doi.org/10.1186/1757-1146-7-19
22. Stindel, E., Udupa, J. K., Hirsch, B. E., Odhner, D., & Couture, C. (1999). 3D MR image analysis of the morphology of the rear foot: application to classification of bones. Computerized medical imaging and graphics, 23(2), 75-83. https://doi.org/10.1016/S0895-6111(98)00070-6
23. Mori, K., Hahn, H. K. (2019). Medical Imaging 2019: Computer-Aided Diagnosis, San Diego, California, United States, 16-21 February 2019. SPIE Proceedings 10950.
24. Park, H. J., Kim, S. M., La Yun, B., Jang, M., Kim, B., Jang, J. Y., ... & Lee, S. H. (2019). A computer-aided diagnosis system using artificial intelligence for the diagnosis and characterization of breast masses on ultrasound: added value for the inexperienced breast radiologist. Medicine, 98(3), e14146. https://doi.org/10.1097/MD.0000000000014146
25. Ben-Cohen, A., & Greenspan, H. (2020). Liver lesion detection in CT using deep learning techniques. In Handbook of medical image computing and computer assisted intervention (pp. 65-90). Academic Press. https://doi.org/10.1016/B978-0-12-816176-0.00008-9
26. Gonzalez, R. C. (2009). Digital image processing. Pearson Education İndia.
27. Beimers, L., Tuijthof, G. J. M., Blankevoort, L., Jonges, R., Maas, M., & van Dijk, C. N. (2008). In-vivo range of motion of the subtalar joint using computed tomography. Journal of biomechanics, 41(7), 1390-1397. https://doi.org/10.1016/j.jbiomech.2008.02.020
28. Mochimaru, M., Kouchi, M., & Dohi, M. (2000). Analysis of 3-D human foot forms using the free form deformation method and its application in grading shoe lasts. Ergonomics, 43(9), 1301-1313. https://doi.org/10.1080/001401300421752
29. Nilsson, M. K., Friis, R., Michaelsen, M. S., Jakobsen, P. A., & Nielsen, R. O. (2012). Classification of the height and flexibility of the medial longitudinal arch of the foot. Journal of foot and ankle research, 5, 1-9. https://doi.org/10.1186/1757-1146-5-3
30. Rodrigo, A. S., Goonetilleke, R. S., & Witana, C. P. (2012). Model based foot shape classification using 2D foot outlines. Computer-Aided Design, 44(1), 48-55. https://doi.org/10.1016/j.cad.2011.01.005
31. Luo, X. D., Xue, C. H., & Li, Y. (2017). Study on the foot shape characteristics of the elderly in China. The Foot, 33, 68-75. https://doi.org/10.1016/j.foot.2017.04.004
32. Reis, H. C., Bayram, B., & Seker, D. Z. (2016). A semiautomatic segmentation approach to biometric measurement of the talus bone of sedentary women and ballerinas using CT images. Asian Biomedicine, 10(5), 455-459. https://doi.org/10.5372/1905-7415.1005.508
33. Goodyear, M. D., Krleza-Jeric, K., & Lemmens, T. (2007). The declaration of Helsinki. British Medical Journal, 335(7621), 624-625. https://doi.org/10.1136/bmj.39339.610000.BE
34. https://www.turkrad.org.tr/
35. Doğan, S., & Altan, M. O. (2010). CT, MR kesitleri ve dijital görüntüler kullanılarak tümörlerin belirlenmesi. İTÜDERGİSİ/d, 2(4), 45-55